Electronic Supplementary Material (ESI) for Materials Chemistry Frontiers.

Supporting Information for

Control of Aggregation-Induced Emission versus Fluorescence Aggregation-Caused Quenching by the Bond Existence at the Single Site in Boron Pyridinoiminate Complexes

Madoka Yamaguchi, Shunichiro Ito, Amane Hirose, Kazuo Tanaka, and Yoshiki Chujo**

Department of Polymer Chemistry, Graduate School of Engineering, Kyoto University, Katsura, Nishikyo-ku, Kyoto 615-8510, Japan

Corresponding authors E-mail: kazuo123@chujo.synchem.kyoto-u.ac.jp; chujo@chujo.synchem.kyoto-u.ac.jp

Tel: (+81)-75-383-2604. Fax: (+81)-75-383-2605

Experimental Section

Measurements: ^{1}H (400 MHz), ^{13}C (100 MHz), and ^{11}B (128 MHz) NMR spectra were recorded on JEOL JNM-EX400 spectrometers. In ^{1}H and ^{13}C NMR spectra, tetramethylsilane (TMS) was used as an internal standard in $CDCl_3$, and ^{11}B NMR spectra were referenced externally to $BF_3{\cdot}OEt_2$ (sealed capillary). TGA was performed on an EXSTAR TG/DTA6220, Seiko Instrument, Inc., with the heating rate of 10 °C/min under nitrogen flowing (200 mL/min). UV−vis spectra were recorded on a SHIMADZU UV-3600 spectrophotometer. Fluorescence emission spectra were measured with a HORIBA JOBIN YVON Fluoromax-4P spectrofluorometer. Cyclic voltammetry (CV) was carried out on a BAS ALS-Electrochemical-Analyzer Model 600D with a glassy carbon working electrode, a Pt counter electrode, an Ag/Ag^{+} reference electrode, and the ferrocene/ferrocenium external reference at a scan rate of 0.05 Vs^{-1}. All reactions were performed under argon. Powder X-ray diffraction (XRD) patterns were taken by using CuKα radiation with a Rigaku Miniflex. X-ray crystallographic analyses were carried out by a Rigaku R-AXIS RAPID-F graphite-monochromated Mo Kα radiation diffractometer with an imaging plate. A symmetry-related absorption correction was carried out by using the program ABSCOR.[1] The analysis was carried out with direct methods (SHELX97[2] or SIR92[3]) using Yadokari-XG[4]. The program ORTEP35 was used to generate the X-ray structural diagram[5]. DSC thermograms were carried out on a SII DSC 6220 instrument. The sample on the aluminum pan was heated at the rate of 10 °C/min under nitrogen flowing (30 mL/min). Elemental analysis was performed at the Microanalytical Center of Kyoto University.

Materials: 2-Methylpyridine (Tokyo Kasei Kogyo, Co.), *N*-methoxy-*N*-methylbenzamide (Tokyo Kasei Kogyo, Co.), aniline (Wako Chemical, Co.), trifluoroacetic acid (Wako Chemical, Co.), 6(5*H*)-phenanthridinone (Tokyo Kasei Kogyo, Co.), phosphorus pentachloride (Tokyo Kasei Kogyo, Co.), *n*-butyllithium (1.64 mol/L in *n*-hexane, Kanto Chemical, Co., Inc.) and boron trifluoride diethyl etherate (BF3·OEt2, Aldrich Chemical, Co.) were used as received. Tetrahydrofuran (THF) and triethylamine were purified using a two-column solid-state purification system (Glasscoutour System, Joerg Meyer, Irvine, CA).

Compound 1a. *n*-Butyllithium (7.2 mL, 11.8 mmol) was added dropwise to the solution of 2-methylpyridine (1 g, 10.7 mmol) in THF (50 mL) at –78 °C under argon atmosphere. The reaction mixture was stirred at –78 °C for 1 h and subsequently at room temperature for 1 h. Next, *N*-methoxy-*N*-methylbenzamide (2.0 g, 10.7 mmol) in THF (50 mL) was added to the solution at –78 °C. After stirring at room temperature for 12 h, the solution was poured into an excess amount of CH_2Cl_2. The solution was washed with brine three times and dried over anhydrous magnesium sulfate. After the solvent was removed by a rotary evaporator, the obtained product was purified by silica gel column chromatography (eluted with hexane/ethyl acetate = 3/2) to give pure **1a** as a yellow solid (1.52 g, 52%). In deuterated chloroform solution, the compound exists as a mixture of keto and enol tautomers. ^{1}H NMR ($CDCl_3$): δ = 8.55 (1H, d, *J* = 4.2 Hz, Ar-*H*, ketone), 8.26 (1H, d, *J* = 5.1 Hz, Ar-*H*, enol), 8.05 (2H, dd, *J* = 8.0, 1.0 Hz, Ar-*H*, ketone), 7.84 (2H, tt, *J* = 6.6, 3.9 Hz, Ar-*H*, enol), 7.63–7.51 (4H, m, Ar-*H*, ketone+enol), 7.45–7.36 (4H, m, Ar-*H*, ketone+enol), 7.28 (1H, d, *J* = 3.9 Hz, Ar-*H*, ketone), 7.14 (1H, m, Ar-*H*, ketone), 7.04 (1H, d, *J* = 8.3 Hz, Ar-*H*, enol), 6.9 (1H, m, Ar-*H*, enol), 6.04 (1H, s, -C*H*=, enol), 4.48 (2H, s, -CH_2-, ketone) ppm. ^{13}C NMR ($CDCl_3$): δ = 196.9, 164.3, 158.6, 155.3, 149.6, 144.3, 137.1, 136.6, 136.5, 133.3, 129.3, 128.8, 128.6, 128.3, 125.5, 124.2, 121.9, 121.6, 118.5, 94.2, 48.4 ppm. HRMS (ESI): Calcd for $[M+H]^+$, 198.0913; found, m/z 198.0911.

Compound 2a. Aniline (0.7 g, 0.69 mL, 7.5 mmol) and trifluoroacetic acid (1 mL) were added to the solution of **1a** (1.5 g, 7.5 mmol) in toluene (30 mL) under argon atmosphere. The reaction mixture was refluxed for 3 h, and the generated water was removed using a Dean-Stark apparatus. After the solvent was removed by a rotary evaporator, the obtained product was poured into an excess amount of CH_2Cl_2. The solution was washed with saturated $NaHCO_3$ solution three times and brine and dried over anhydrous magnesium sulfate. After the solvent was removed by a rotary evaporator, the obtained product was purified by silica gel column chromatography (eluted with hexane/ethyl acetate = 3/1) to give pure **2a** as a yellow solid (1.5 g, 74%). ^{1}H NMR ($CDCl_3$): δ = 11.7 (1H, s, -N*H*-), 7.78 (1H, d, *J* = 3.9 Hz, Ar-*H*), 7.50−7.45 (3H, m, Ar-*H*), 7.29−7.25 (3H, m, Ar-*H*), 7.06−7.02 (3H, m, Ar-*H*), 6.86 (1H, m, Ar-*H*), 6.78 (1H, t, *J* = 14.6 Hz, Ar-*H*), 6.68 (2H, d, *J* = 7.8 Hz, Ar-*H*), 5.57 (1H, s, -C*H*=) ppm. ^{13}C NMR ($CDCl_3$): δ = 158.6, 148.4, 147.3, 142.4, 138.2, 135.9, 128.5, 128.3, 128.2, 128.0, 122.9, 120.9, 120.8, 118.4, 103.5 ppm. HRMS (NSI): Calcd for $[M+H]^+$, 273.1386; found, m/z 273.1382.

BPI. $BF_3{\cdot}OEt_2$ (6.8 mL, 7.8 g, 55.1 mmol) and triethylamine (7.7 mL, 5.6 g, 55.1 mmol) were added to the solution of **2a** (1.5 g, 5.5 mmol) in toluene (30 mL) at ambient temperature, and the solution was stirred at 100 °C for 12 h. After precipitates were removed by filtration, the solvent was removed by a rotary evaporator. The obtained product was purified by silica gel column chromatography (eluted with hexane/ethyl acetate = 3/1). The product was purified by recrystallization from methanol. The precipitate collected by filtration was dried *in vacuo* to give pure **BPI** as a yellow crystal (1.3 g, 25%). ^{1}H NMR ($CDCl_3$): δ = 8.33 (1H, d, *J* = 6.1 Hz, Ar-*H*), 7.69 (1H, m, Ar-*H*), 7.30−7.25 (2H, m, Ar-*H*), 7.20−7.16 (4H, m, Ar-*H*), 7.13−7.09 (2H, m, Ar-*H*), 7.06−7.04 (3H, m, Ar-*H*), 6.99 (1H, m, Ar-*H*), 5.71 (1H, s, -C*H*=) ppm. ^{13}C NMR ($CDCl_3$): δ = 157.5, 151.0, 142.8, 138.7, 138.6, 137.6, 129.1, 128.6, 128.1, 127.9, 127.7, 124.7, 122.1, 117.1, 95.5 ppm. ^{11}B NMR ($CDCl_3$): δ = 1.95 (t, *J* = 31.3 Hz) ppm. HRMS (ESI): Calcd for $[M+H]^+$, 321.1369; found, m/z 321.1364. Anal. Calcd for $C_{19}H_{15}BF_2N_2$: C, 71.28; H, 4.72; N, 8.75. Found: C, 71.12; H, 4.65; N, 8.70.

Compound 1b. Phosphorus pentachloride (6.2 g, 29.9 mmol) was added to the solution of 6(5*H*)-phenanthridinone (5.3 g, 27.2 mmol) in toluene (60 mL). The reaction mixture was stirred under argon atmosphere at 100 °C for 24 h. After the solution was cooled to ambient temperature, the solvent was removed by vacuum distillation. Sodium hydrogen carbonate and toluene were added to the residue for neutralization. Precipitates were removed by filtration, and then the solvent was removed by a rotary evaporator to give desired product **1b** as a pale yellow solid (1.4 g, 86%). The product was used for the next reaction without further purification.

Compound 2b. *n*-Butyllithium (15.3 mL, 23.6 mmol) was added dropwise to the solution of 2-methylpyridine (2 g, 21.5 mmol) in THF (50 mL) at –78 °C under argon atmosphere. The reaction mixture was stirred at –78 °C for 1 h and additionally at room temperature for 2 h. Next, **1b** (4.6 g, 21.5 mmol) in THF (50 mL) was added to the solution at –78 °C. After stirring at room temperature for 12 h, the solution was poured into an excess amount of CH_2Cl_2. The solution was washed with brine three times and dried over anhydrous magnesium sulfate. After the solvent was removed by a rotary evaporator, the obtained product was purified by silica gel column chromatography (eluted with hexane/ethyl acetate = 1/1) to give pure **2b** as a yellow solid. (1.7 g, 29%). ^{1}H NMR ($CDCl_3$): δ = 8.54−8.45 (3H, m, Ar-*H*), 8.32 (1H, d, *J* = 8.3 Hz, Ar-*H*), 8.18 (1H, d, *J* = 8.0 Hz, Ar-*H*), 7.71−7.67 (2H, m, Ar-*H*), 7.11 (2H, tt, *J* = 19.8, 15.4 Hz, Ar-*H*), 7.41 (1H, t, *J* = 13.9 Hz, Ar-*H*), 7.19 (1H, d, *J* = 8.0 Hz, Ar-*H*), 7.02 (1H, t, *J* = 12.2 Hz, Ar-*H*), 4.93 (2H, s, -C*H*$_2$-) ppm. ^{13}C NMR ($CDCl_3$): δ = 159.1, 159.1, 149.1, 143.6, 136.3, 133.0, 130.2, 129.7, 128.5, 127.2, 127.2, 126.6, 125.4, 123.8, 123.1, 122.1, 121.8, 121.3, 46.2 ppm. HRMS (ESI): Calcd for $[M+H]^+$, 271.1230; found, m/z 271.1223.

FBPI. $BF_3{\cdot}OEt_2$ (5.5 mL, 6.3 g, 44.4 mmol) and triethylamine (6.2 mL, 4.5 g, 44.4 mmol) were added to the solution of **2b** (1.2 g, 4.4 mmol) in toluene (50 mL) at ambient temperature, and the solution was stirred at 100 °C for 12 h. After precipitates were removed by filtration, the solvent was removed by a rotary evaporator. The obtained product was dissolved in a small amount of $CHCl_3$, and then the product was reprecipitated from methanol. The product was purified by recrystallization from $CHCl_3$ and hexane. The precipitate collected by filtration was dried in vacuum to give pure **FBPI** as a red crystal (1.2 g, 90%). ^{1}H NMR ($CDCl_3$): δ = 8.40 (1H, m, Ar-*H*), 8.27−8.22 (2H, m, Ar-*H*), 8.18 (1H, d, *J* = 8.2 Hz, Ar-*H*), 8.14

(1H, d, *J* = 8.6 Hz, Ar-*H*), 7.64 (1H, t, *J* = 15.4 Hz, Ar-*H*), 7.54−7.45 (3H, m, Ar-*H*), 7.25 (1H, t, *J* = 15.1 Hz, Ar-*H*), 7.07 (1H, d, *J* = 8.0 Hz, Ar-*H*), 6.84 (1H, t, *J* = 13.4 Hz, Ar-*H*), 6.28 (1H, s, -C*H*=) ppm. ^{13}C NMR ($CDCl_3$): δ = 149.8, 147.5, 138.6, 138.0, 137.7, 131.8, 131.1, 129.4, 129.29, 127.9, 125.6, 125.5, 124.8, 123.0, 122.2, 121.6, 121.2, 114.8, 85.4 ppm. ^{11}B NMR ($CDCl_3$): δ = 3.23 (t, *J* = 37.5 Hz) ppm. HRMS (ESI): Calcd for $[M+H]^+$, 319.1213; found, m/z 319.1204. Anal. Calcd for $C_{19}H_{13}BF_2N_2$: C, 71.73; H, 4.12; N, 8.81. Found: C, 71.62; H, 4.14; N, 8.69.

(a)

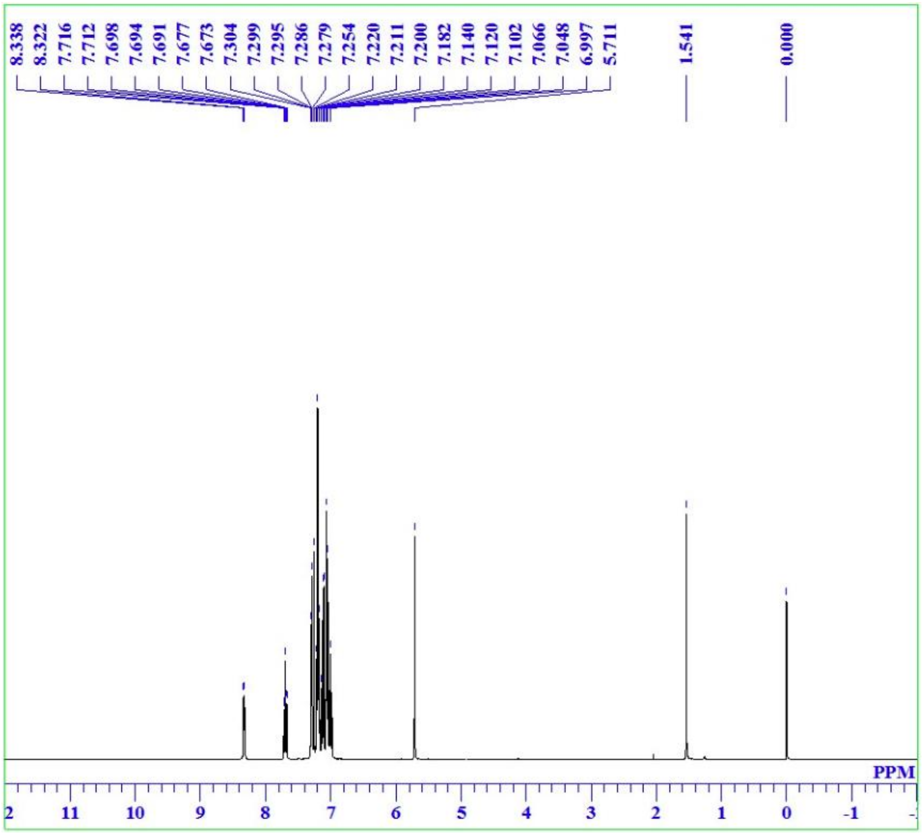
8.338
8.322
7.716
7.712
7.698
7.694
7.691
7.677
7.673
7.304
7.299
7.295
7.286
7.279
7.254
7.220
7.211
7.200
7.182
7.140
7.120
7.102
7.066
7.048
6.997
5.711
1.541
0.000
PPM
2
11
10
9
8
7
6
5
4
3
2
1
0
-1

(b)

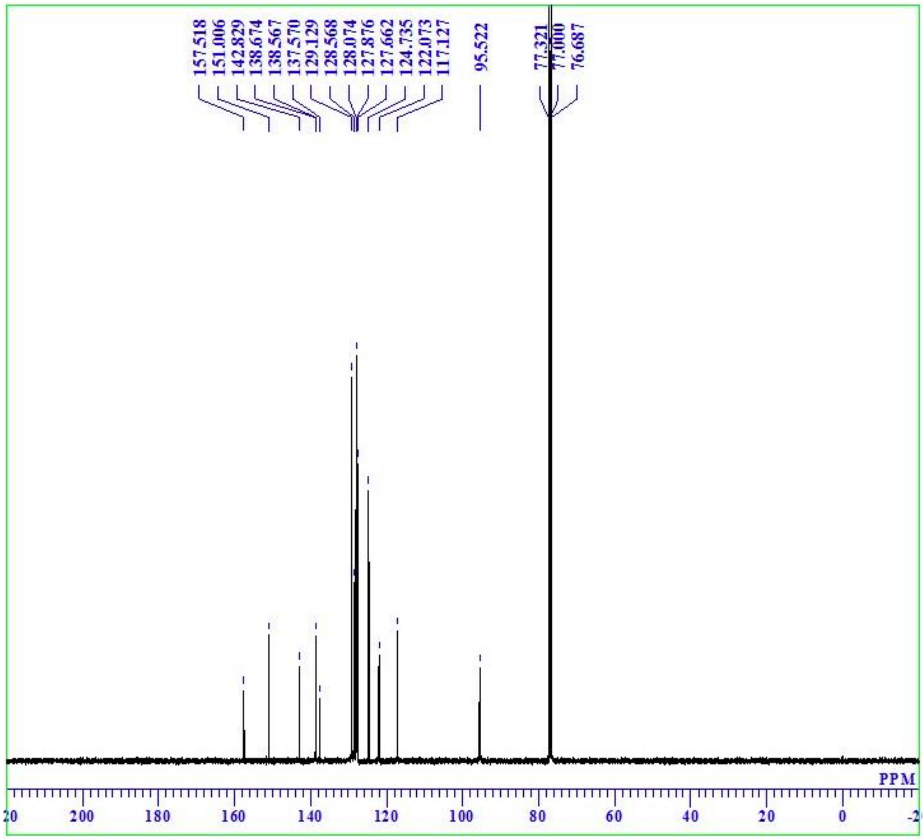
157.518
151.006
142.829
138.674
138.567
137.570
129.129
128.568
128.074
127.876
127.662
124.735
122.073
117.127
95.522
77.321
77.000
76.687
PPM
20
200
180
160
140
120
100
80
60
40
20
0

(c)

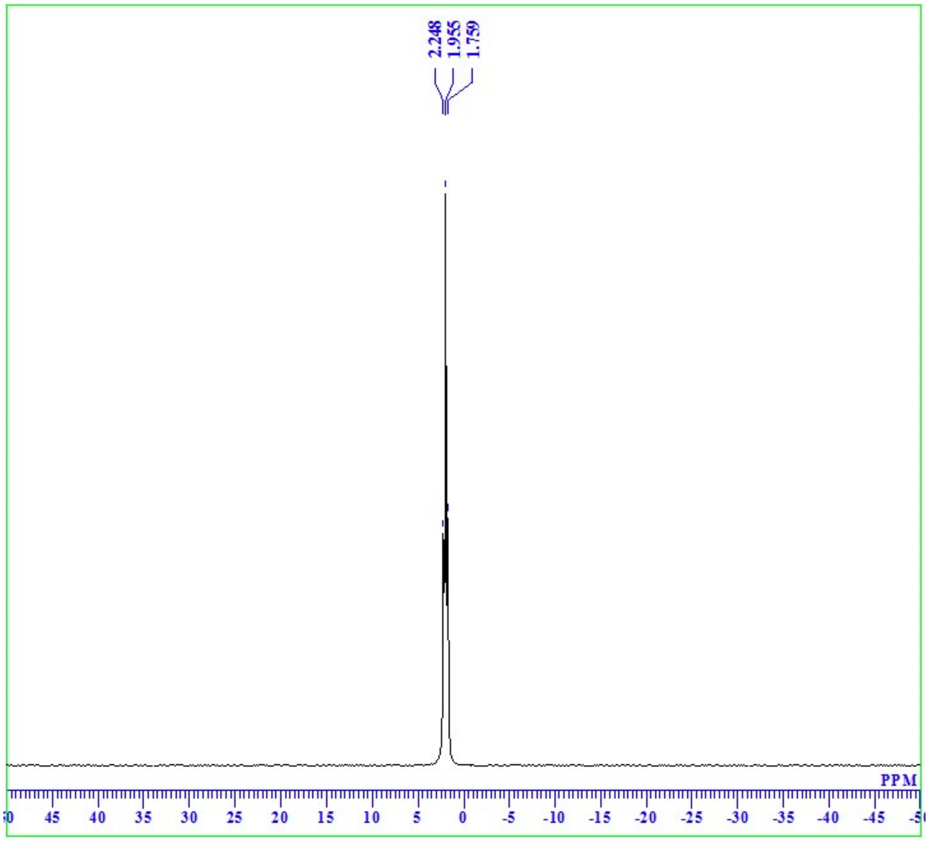

Figure S1. (a) ^{1}H, (b) ^{13}C and (c) ^{11}B NMR spectra of **BPI** in $CDCl_3$.

(a)

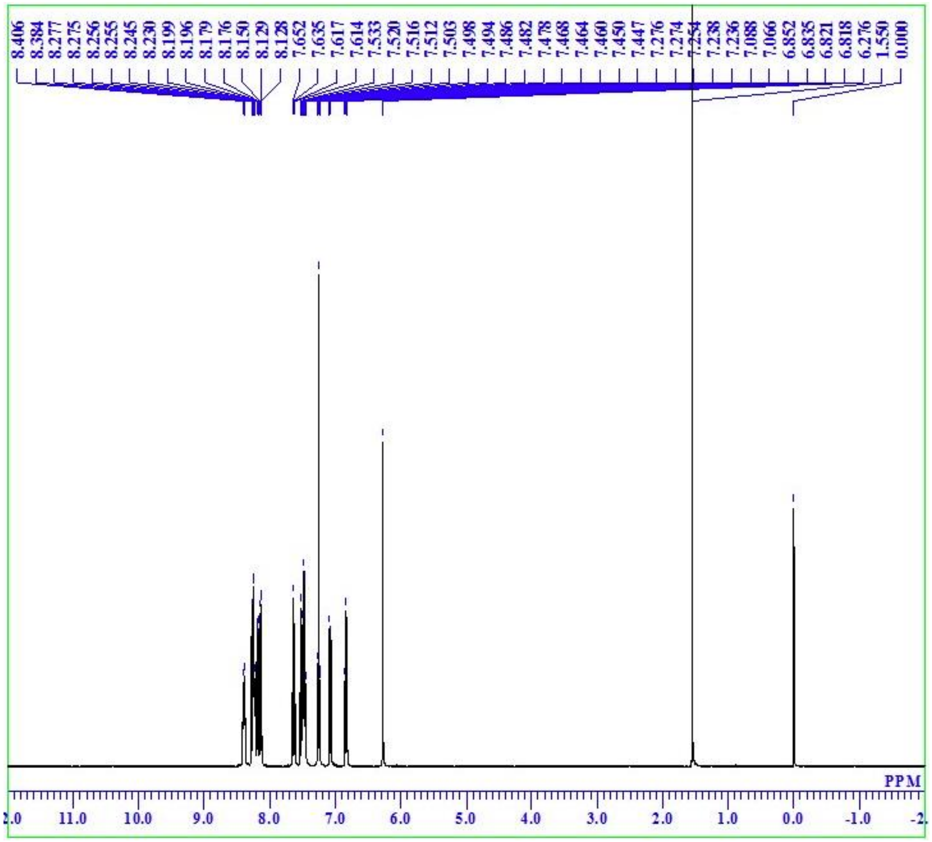
8.406
8.384
8.277
8.275
8.256
8.255
8.245
8.230
8.199
8.196
8.179
8.176
8.150
8.129
8.128
7.652
7.635
7.617
7.614
7.533
7.520
7.516
7.512
7.503
7.498
7.494
7.486
7.482
7.478
7.468
7.464
7.460
7.450
7.447
7.276
7.274
7.254
7.238
7.236
7.088
7.066
6.852
6.835
6.821
6.818
6.276
1.550
0.000
PPM
11.0
10.0
9.0
8.0
7.0
6.0
5.0
4.0
3.0
2.0
1.0
0.0
-1.0

(b)

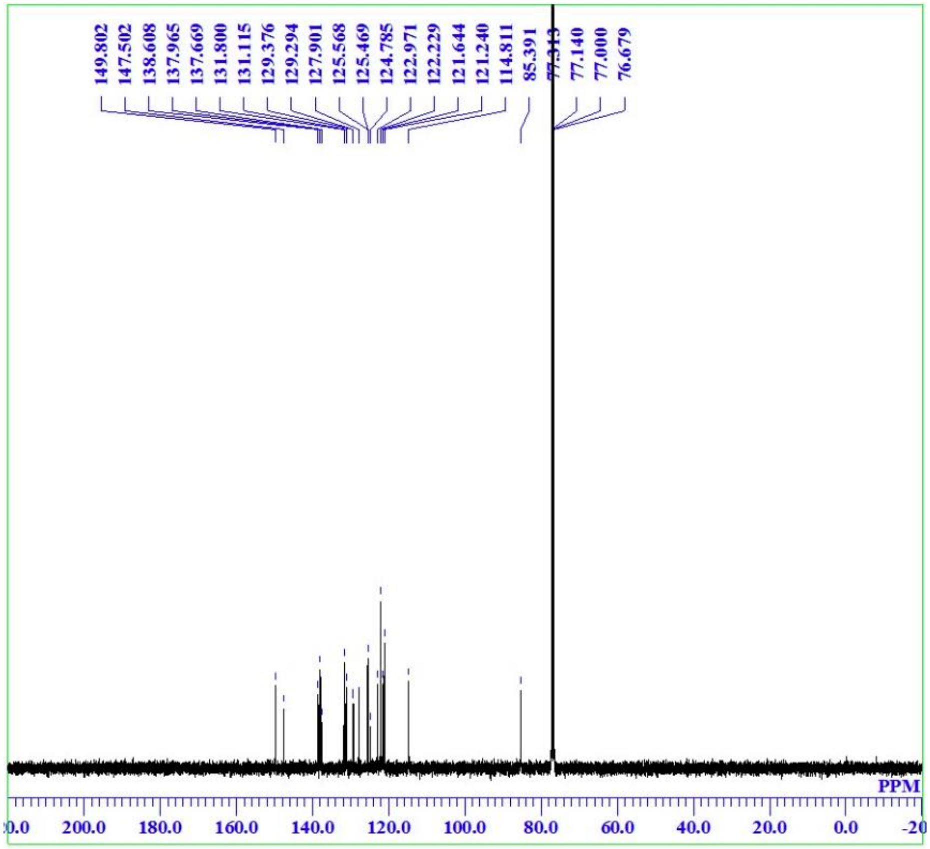
149.802
147.502
138.608
137.965
137.669
131.800
131.115
129.376
129.294
127.901
125.568
125.469
124.785
122.971
122.229
121.644
121.240
114.811
85.391
77.313
77.140
77.000
76.679
PPM
200.0
180.0
160.0
140.0
120.0
100.0
80.0
60.0
40.0
20.0
0.0

(c)

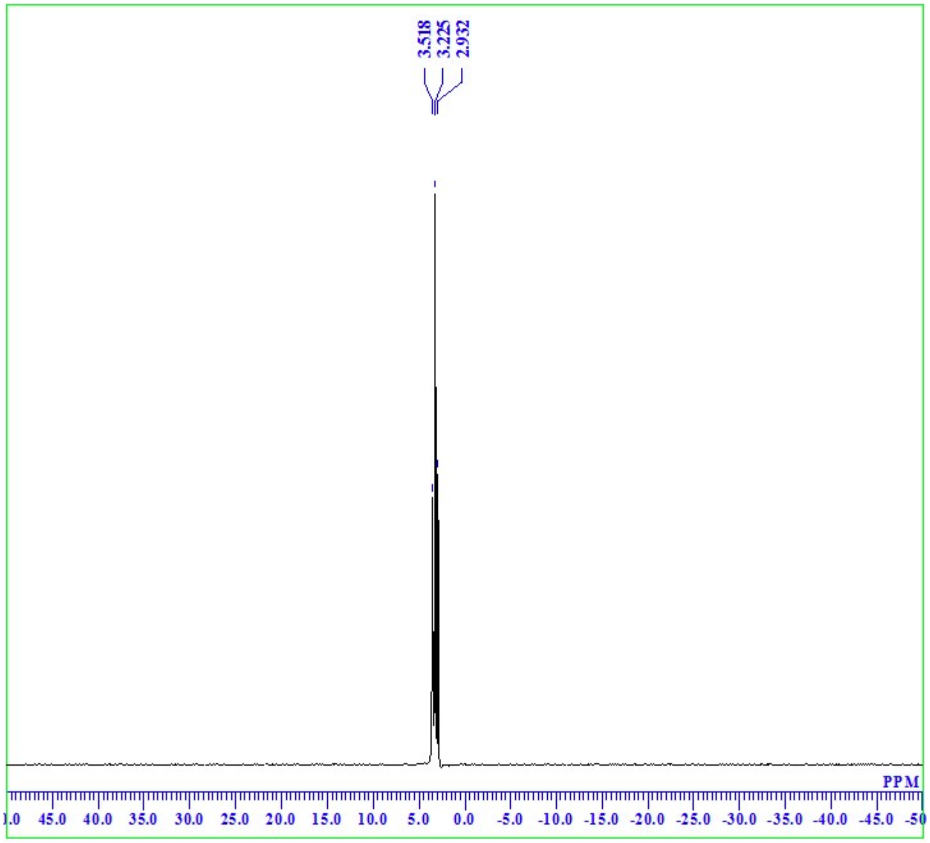

Figure S2. (a) ^{1}H, (b) ^{13}C and (c) ^{11}B NMR spectra of **FBPI** in $CDCl_3$.

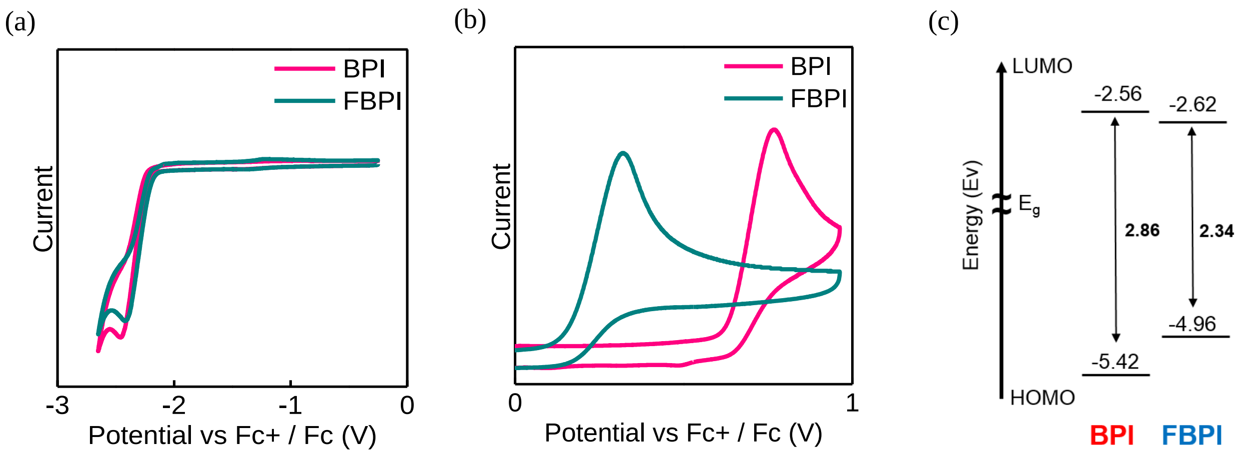

Figure S3. Cyclic voltammograms of **BPI** and **FBPI** from (a) 0 V to −2.4 V (b) 0 V to 1.2 V in CH_2Cl_2 (1.0×10^{-3} M) with 0.1 M Bu_4NPF_6 as a supporting electrolyte, AgCl/Ag as a reference electrode, Pt as working and counter electrodes, and scan rate at 100 mV/s. (c) Energy diagrams of **BPI** and **FBPI** calculated by CV measurements.

Table S1. Electrochemical results with **BPI** and **FBPI** from CV measurements

	E_{Ox} [a] [V]	E_{red} [b] [V]	HOMO[c] [eV]	LUMO[d] [eV]
BPI	0.62	−2.24	−5.42	−2.56
FBPI	0.16	−2.18	−4.96	−2.62

[a] E_{Ox} is the onset potential of first oxidation wave.
[b] E_{red} is the onset potential of first reduction wave.
[c] Calculated from the empirical formula[6], HOMO = $-E_{\mathrm{Ox}} - 4.80$ (eV).
[d] Calculated from the empirical formula[6], LUMO = $-E_{\mathrm{red}} - 4.80$ (eV).

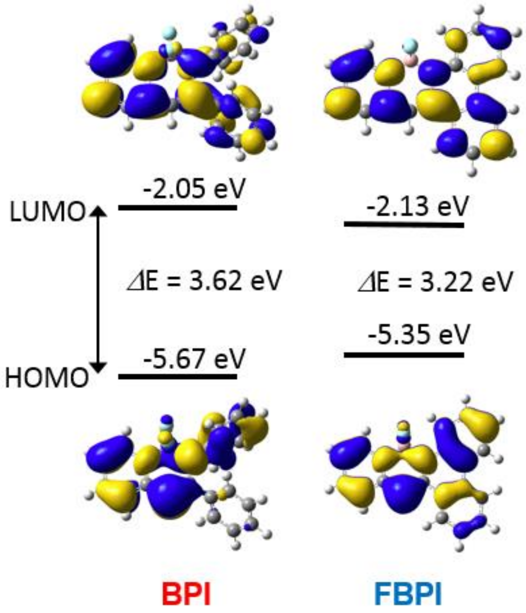

Figure S4. Structures and molecular orbital diagrams for the LUMO and HOMO of **BPI** and **FBPI** ((B3LYP/6-31G+ (d, p)//B3LYP/6-31G+ (d, p)).

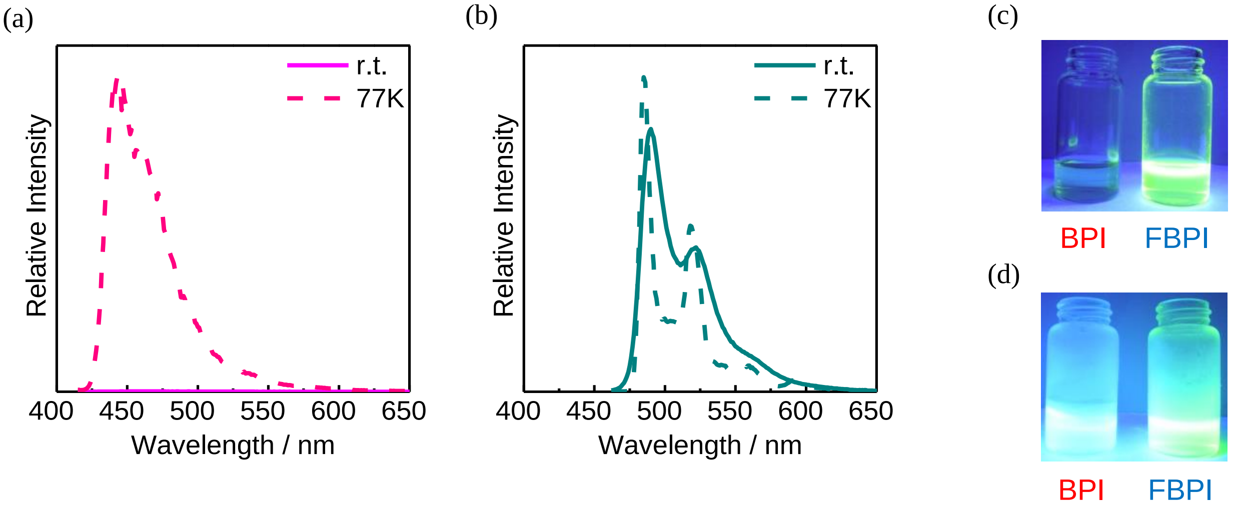

Figure S5. PL spectra of (a) **BPI** and (b) **FBPI** in 2-Me-THF (1.0×10^{-5} M) at r.t. (solid line) and at 77 K (dashed line). (c) Photographs of **BPI** and **FBPI** in 2-Me-THF (1.0×10^{-5} M) at r.t. under UV irradiation. (d) Photographs of **BPI** and **FBPI** in 2-Me-THF (1.0×10^{-5} M) at 77 K under UV irradiation.

Table S2. PL properties of **BPI** and **FBPI** in 2-Me-THF (1.0×10^{-5} M)

	$\lambda_{\mathrm{PL,\ r.t.}}$ [nm]	$\lambda_{\mathrm{PL,\ 77K}}$ [nm]
BPI	459	443
FBPI	490	485

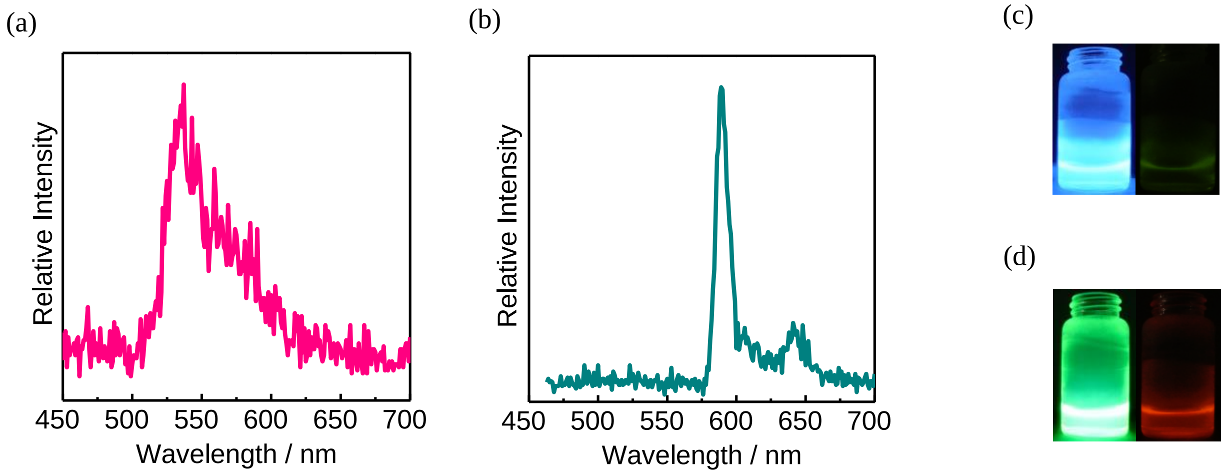

Figure S6. PL spectra of (a) **BPI** and (b) **FBPI** in 2-Me-THF (1.0×10^{-5} M) at 77 K delayed after 1 ms. (c) Photographs of **BPI** in 2-Me-THF (1.0×10^{-5} M) at 77K under UV irradiation and immediately after tuning off UV irradiation. (d) Photographs of **FBPI** in 2-Me-THF (1.0×10^{-5} M) at 77 K under UV irradiation and immediately after tuning off UV irradiation.

Table S3. Phosphorescence properties of **BPI** and **FBPI** in 2-Me-THF (1.0×10^{-5} M) at 77K

	λ_{PL} [nm]
BPI	537
FBPI	589

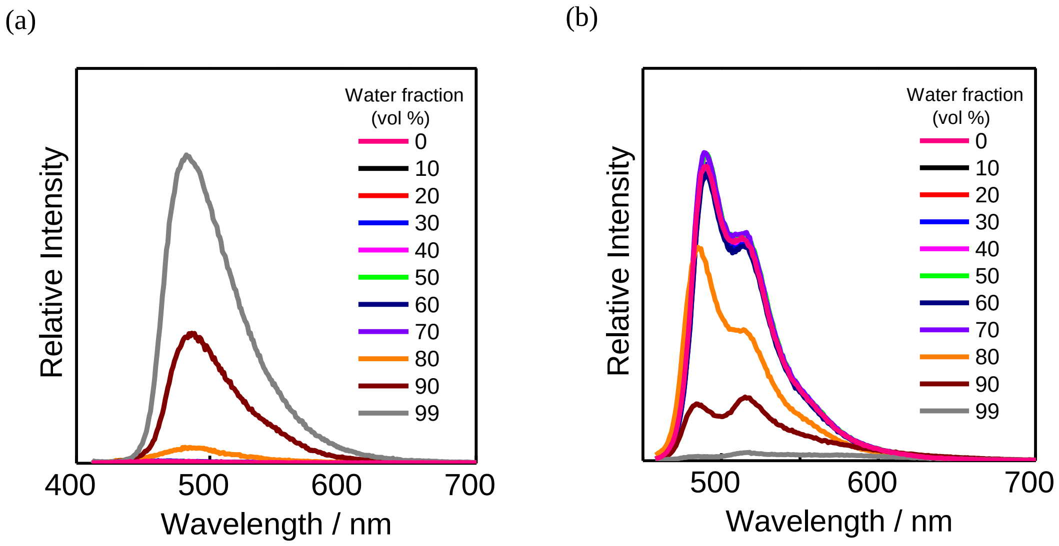

Figure S7. PL spectra of (a) **BPI** and (b) **FBPI** in acetonitrile / H_2O mixture solvents (1.0×10^{-4} M).

Front view ***Side view***

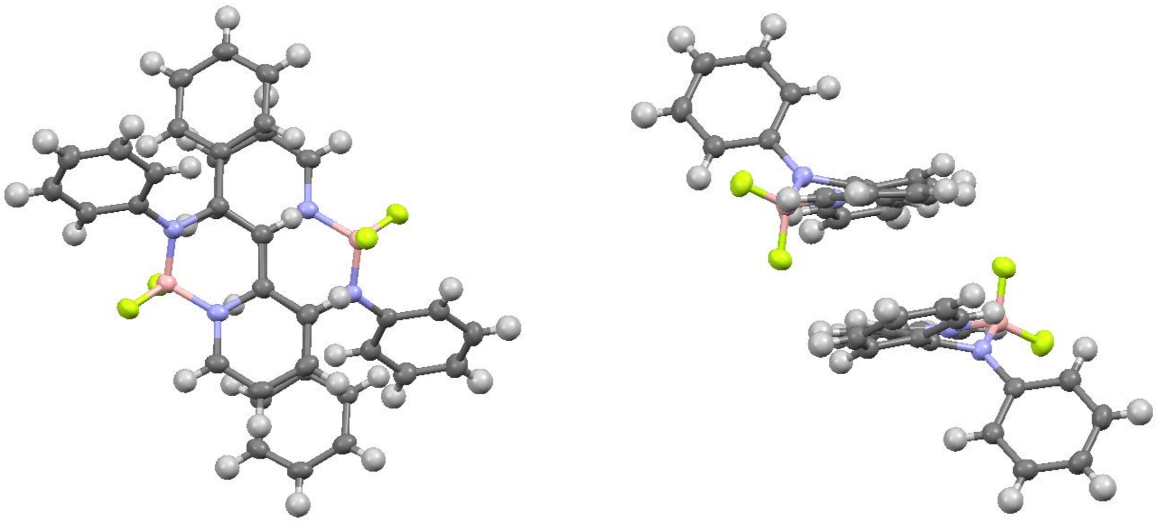

Packing structure

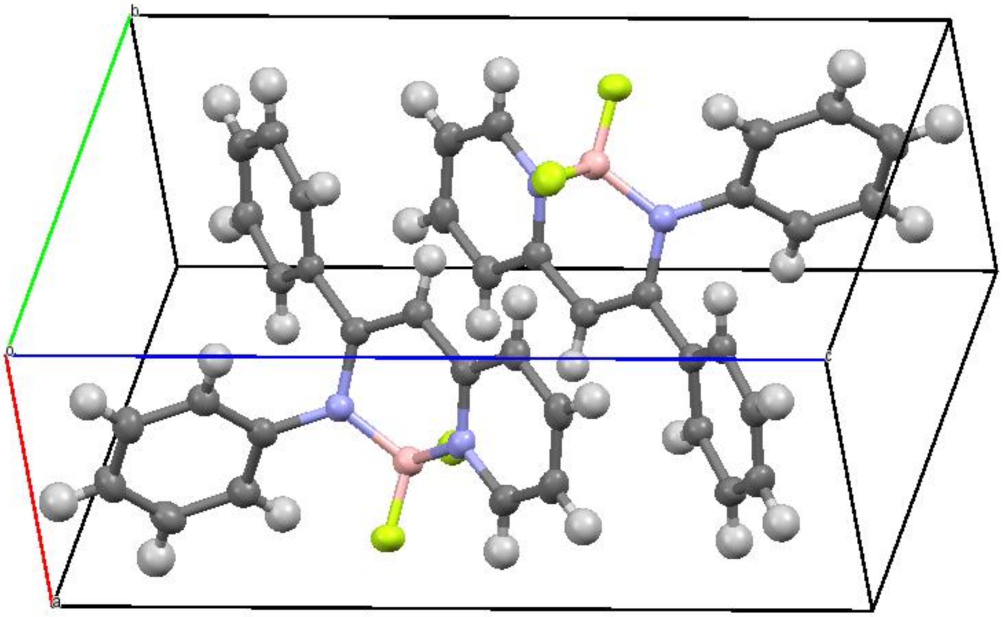

Figure S8. ORTEP drawings of the **BPI** dimer and the packing structures.

Table S4. Crystallographic data of **BPI**[a]

Empirical formula	$C_{19}H_{15}BF_2N_2$
Formula weight	320.14
Temperature (K)	93(2)
Wavelength (Å)	0.71075
Crystal system, space group	triciclinic, *P* -1
Unit cell dimensions	a = 6.418(3)
	b = 8.632(4)
	c = 14.198(6)
	α = 74.951(6)
	β = 81.658(7)
	γ = 751.3(6)
V (Å^3)	751.3(6)
Z, calculated density (Mg m^{-3})	2, 1.415
Absorption coefficient	0.100
F(000)	332
Crystal size (mm)	0.10 × 0.10 × 0.10
θ range for data collection	3.175 –27.485
Limiting indices	$-8 \leq h \leq 8$, $-10 \leq k \leq 11$, $-17 \leq l \leq 18$
Reflections collected (unique)	6456/3230 [R(int) = 0.0818]
Completeness to theta = 27.48	0.985
Goodness-of-fit on F^2	1.036
Final R indices [$I > 2\sigma(I)$][b]	R_1 = 0.0596, wR_2 = 0.1541
R indices (all data)	R_1 = 0.0713, wR_2 = 0.1623

---

[a] The structures were solved by direct method (SIR97) and refined by full-matrix least-squares procedures based on F^2 (SHELX-97). [b] $R_1 = \Sigma(|F_0|-|F_c|)/\Sigma|F_0|$. $wR_2 = [\Sigma w(F^2{}_0-F^2{}_c)^2/\ \Sigma w(F^2{}_0)^2]^{1/2}$. $w = 1/[\sigma^2(F^2{}_0)+[(ap)^2+bp]]$, where $p = [\max(F^2{}_0,0)+2F^2{}_c]/3$.

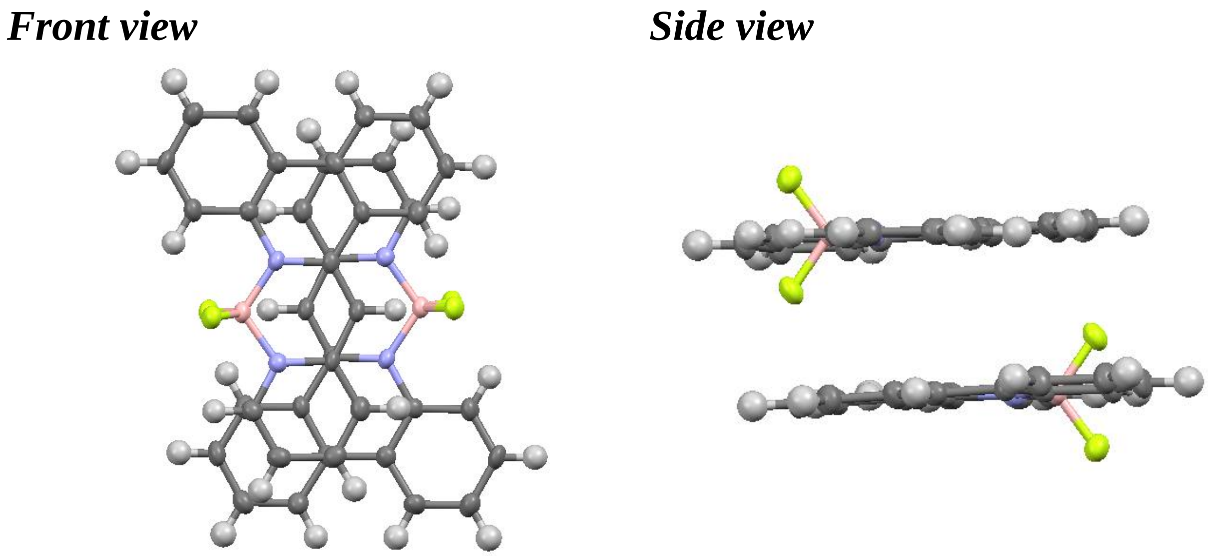
Front view

Side view

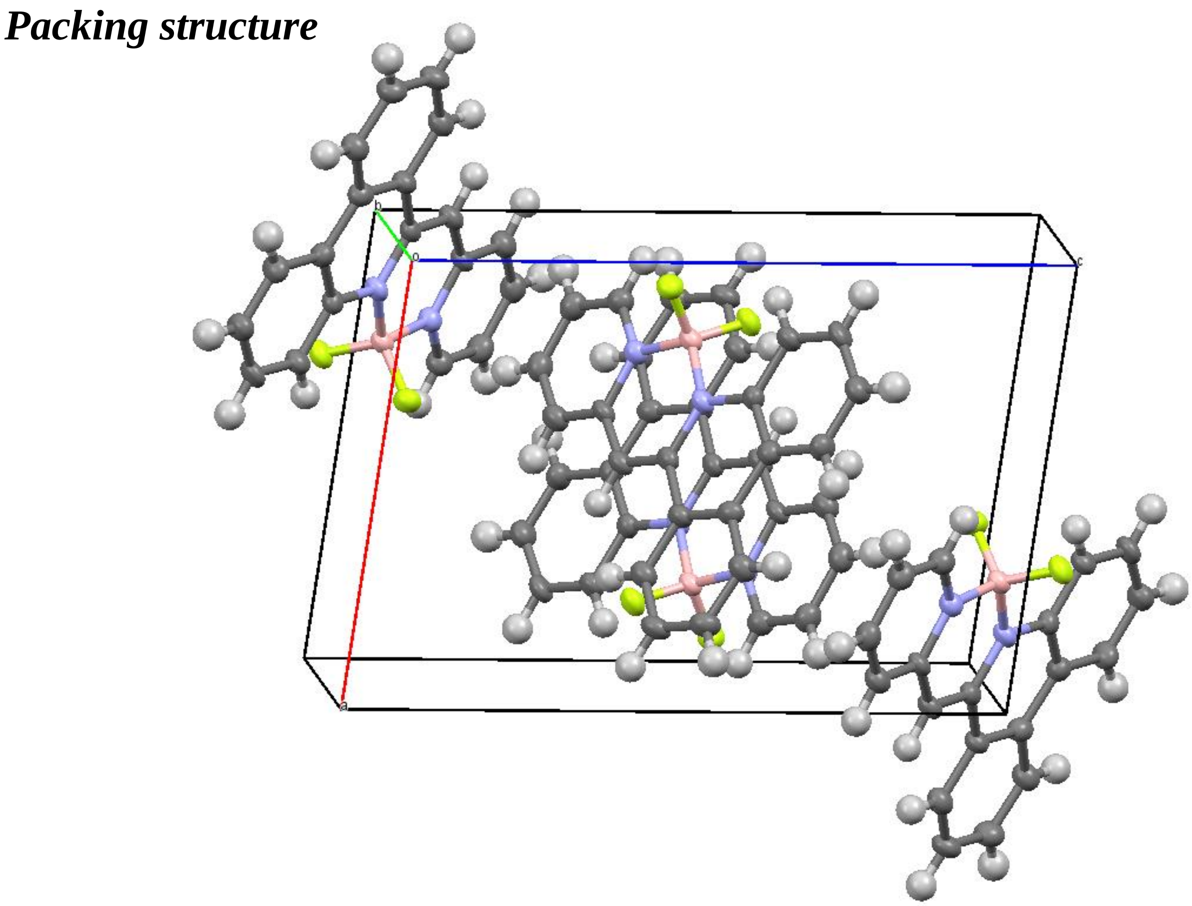
Packing structure

Figure S9. ORTEP drawings of the **FBPI** dimer and the packing structures.

Table S5. Crystallographic data of **FBPI**[a]

Empirical formula	$C_{19}H_{13}BF_2N_2$
Formula weight	318.12
Temperature (K)	93(2)
Wavelength (Å)	0.71075
Crystal system, space group	monoclinic, $P\ 2_1/n$
Unit cell dimensions	a = 9.2376(8)
	b = 11.5433(11)
	c = 13.4497(11)
	α = 90
	β = 98.264(7)
	γ = 90
V (Å^3)	1419.3(2)
Z, calculated density (Mg m^{-3})	4, 1.489
Absorption coefficient	0.106
F(000)	656
Crystal size (mm)	0.10 × 0.10 × 0.10
θ range for data collection	3.061 –27.477
Limiting indices	$-10 \leq h \leq 11$, $-14 \leq k \leq 14$, $-17 \leq l \leq 17$
Reflections collected (unique)	13004/5674 [R(int) = 0.0646]
Completeness to theta = 27.48	0.996
Goodness-of-fit on F^2	1.087
Final R indices [$I > 2\sigma(I)$][b]	R_1 = 0.0490, wR_2 = 0.1448
R indices (all data)	R_1 = 0.0627, wR_2 = 0.1720

[a] The structures were solved by direct method (SIR97) and refined by full-matrix least-squares procedures based on F^2 (SHELX-97). [b] $R_1 = \Sigma(|F_0|-|F_c|)/\Sigma|F_0|$. $wR_2 = [\Sigma w(F^2{}_0-F^2{}_c)^2/\ \Sigma w(F^2{}_0)^2]^{1/2}$. $w = 1/[\sigma^2(F^2{}_0)+[(ap)^2+bp]]$, where $p = [\max(F^2{}_0,0)+2F^2{}_c]/3$.

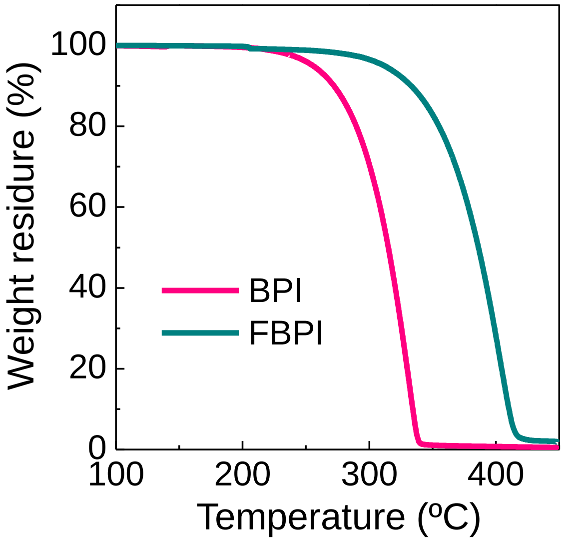

Figure S10. TGA profiles of **BPI** and **FBPI**.

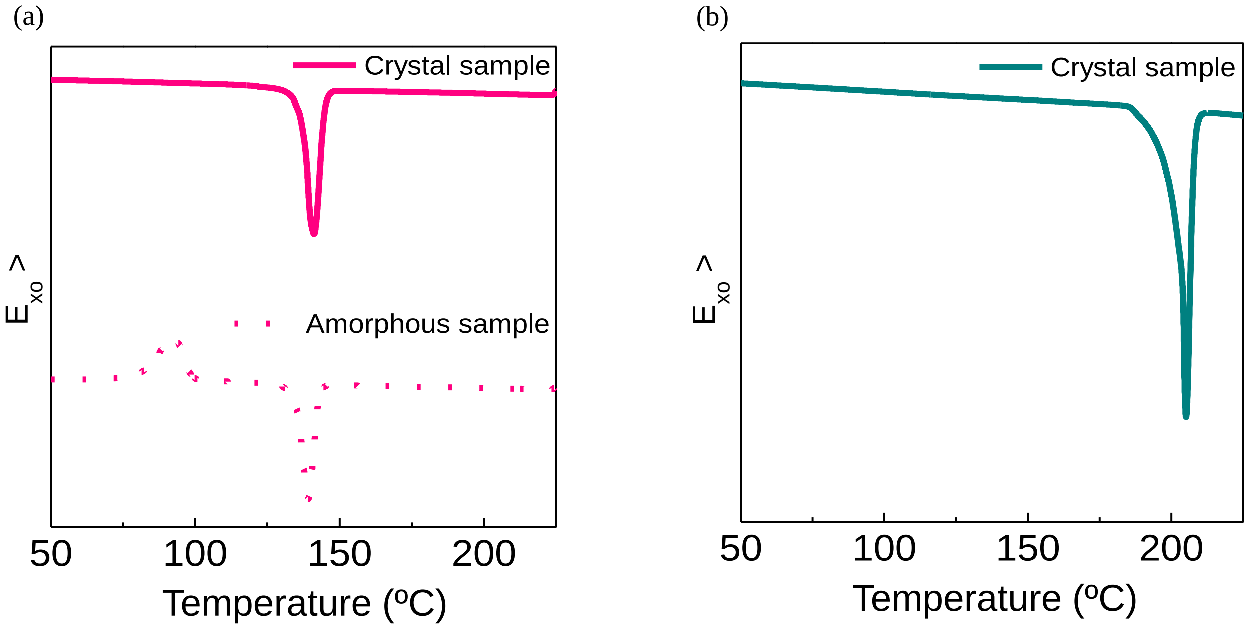

Figure S11. DSC profiles of (a) **BPI** and (b) **FBPI**.

Table S6. Thermal properties of **BPI** and **FBPI**

	T_{5d}[a]	T_{cr}	T_{m}
BPI	256	92	141
FBPI	312	-	205

[a] Decomposition temperature with 5 wt% weight losses.

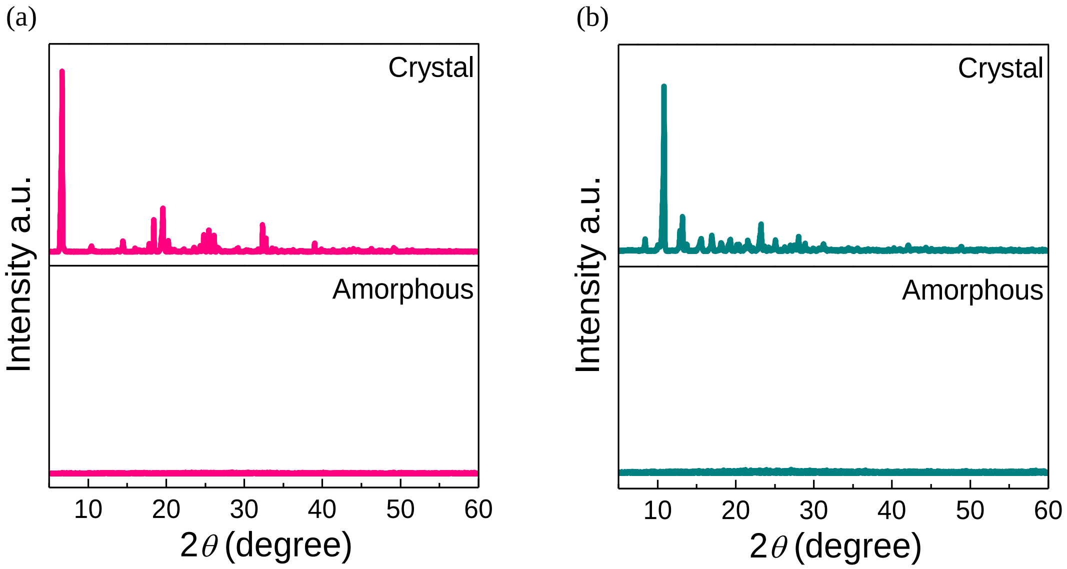

Figure S12. XRD patterns of (a) **BPI** and (b) **FBPI** crystalline and amorphous states.

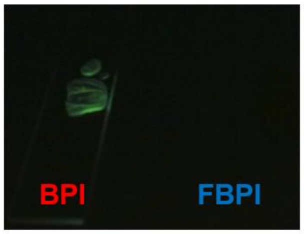

Figure S13. Photographs of **BPI** and **FBPI** in the amorphous state under UV irradiation.

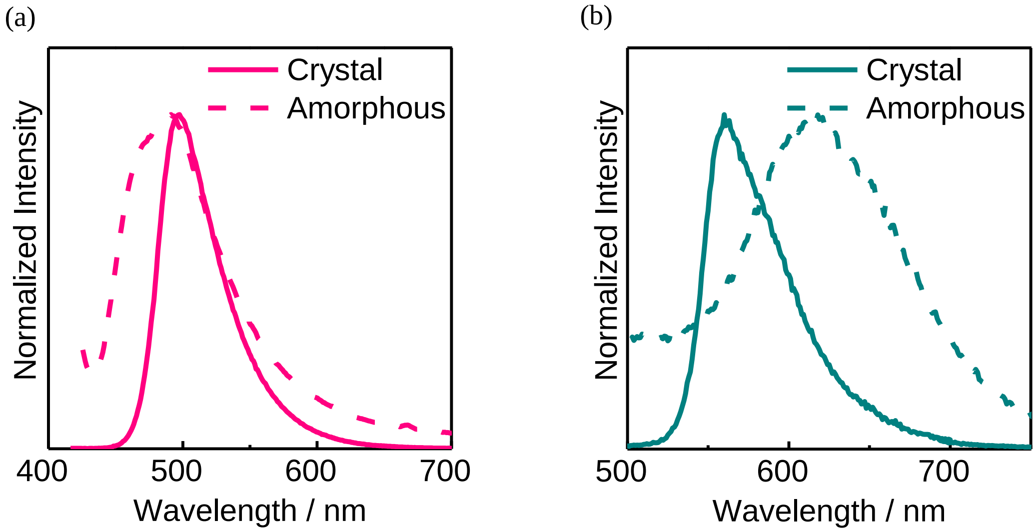

Figure S14. PL spectra of (a) **BPI** and (b) **FBPI** in crystalline and amorphous states.

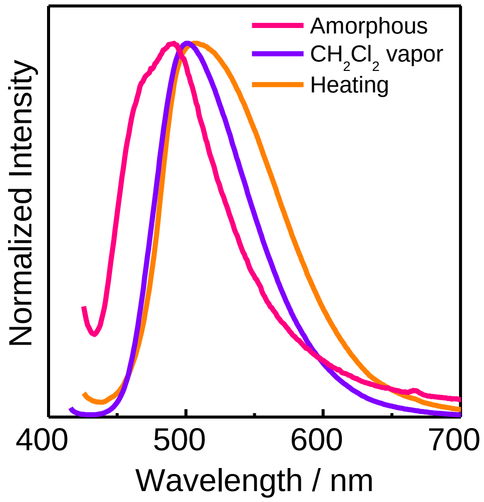

Figure S15. PL spectra of amorphous and crystalline (CH_2Cl_2 vapor or heating) samples of **BPI.**

Table S7. PL properties of amorphous and crystal (CH_2Cl_2 vapor or heating) samples of **BPI**

	λ_{PL} (amorphous) [nm]	λ_{PL} (CH_2Cl_2 vapor) [nm]	λ_{PL} (heating) [nm]
BPI	491	502	506

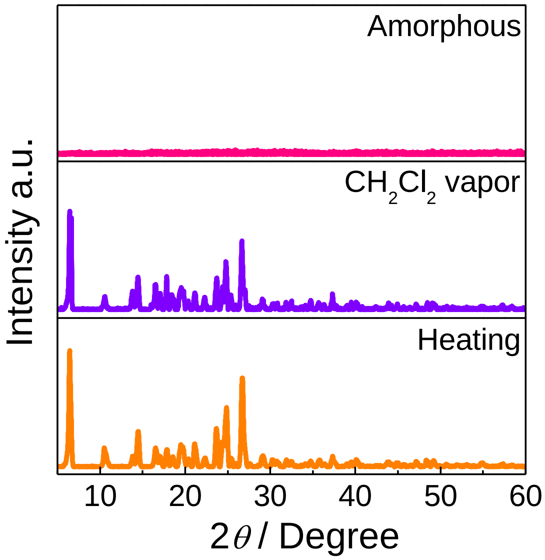

Figure S16. XRD patterns of amorphous and the treated (CH_2Cl_2 vapor or heating) samples of **BPI.**

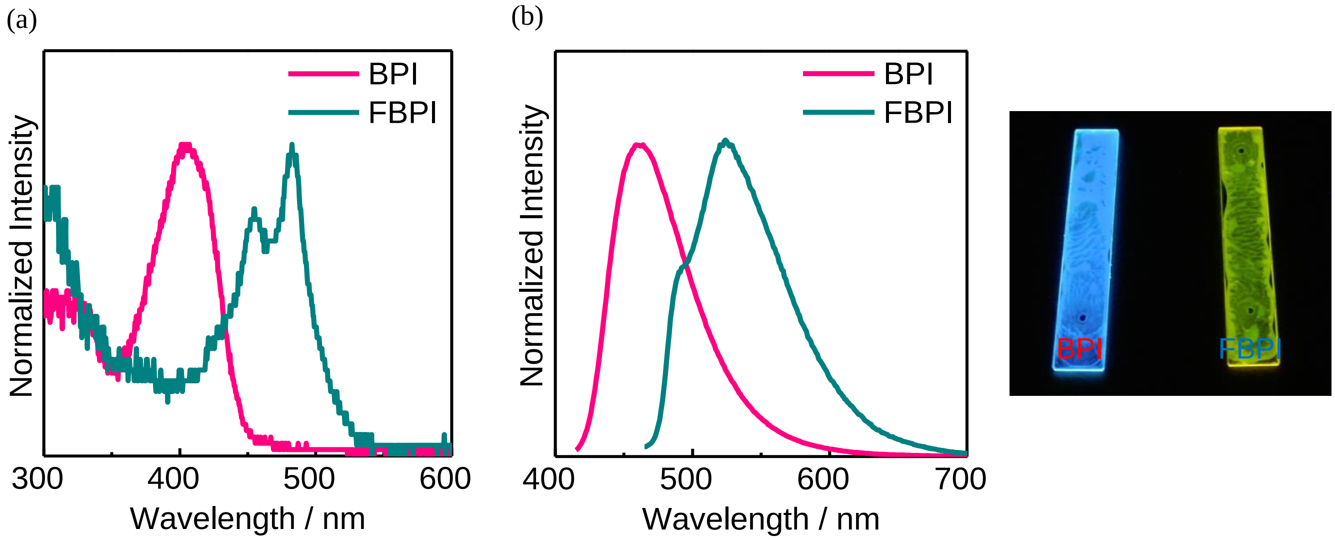

Figure S17. (a) UV−vis absorption and (b) PL spectra of **BPI** and **FBPI** in a polymer matrix (1 wt% in PMMA). (c) Photographs under UV irradiation.

Table S8. PL properties of **BPI** and **FBPI** in a polymer matrix

	λ_{abs} [nm]	λ_{PL} [nm]	$\Phi_{\mathrm{PL}}{}^{c}$	τ^{d} [ns]	
BPI	404	464[a]	0.31	2.72 (52%)	5.78 (48%)
FBPI	483	520[b]	0.35	3.2 (44%)	5.87 (56%)

[a] Excited at λ_{abs}.

[b] Excited at 453 nm.

[c] Determined as an absolute value.

[d] Excited at 375 nm.

References

1) Higashi, T. ABSCOR. Program for Absorption Correction.; Rigaku Corporation: Japan, **1995**.

2) Sheldrick, G. M. SHELX–97. Programs for Crystal Structure Analysis; University of Göttingen: Germany, **1997**.

3) Altomare, A.; Burla, M. C.; Camalli, M.; Cascarano, G. L.; Giacovazzo, C.; Guagliardi, A.; Moliteri, A. G. G.; Polidori, G.; Spagna, R. *J. Appl. Cryst*. **1999**, *32*, 115.

4) Wakita, Y. Yadokari–XG. Program for Crystal Structure Analysis.; **2000**.

5) Farrugia, L. *J. Appl. Cryst*. **1997**, *30*, 565.

6) Chen, C.-P.; Chan, S.-H.; Chao, T.-C.; Ting, C.; Ko, B.-T. *J. Am. Chem. Soc.* **2008**, *130*, 12828.